Stabilized Multi-Hop Route Construction Using a Modified Link Metric for Wi-SUN FAN Systems

Ryuichi Nagao, *Student Member*, *IEEE,* Daiki Hotta, Hiroko Masaki, *non-Members*, *IEEE*, Keiichi Mizutani, *Member*, *IEEE*, and Hiroshi Harada, *Fellow, IEEE*

Abstract Wireless Smart Utility Network Field Area Network (Wi-SUN FAN) is a technical specification of Wi-SUN that introduces multi-hop machine-to-machine transmission for advanced smart city infrastructure. Wi-SUN FAN uses the Internet Protocol Version 6 (IPv6) Routing Protocol for Low-Power and Lossy Network (RPL) as the routing protocol and expected transmission count (ETX) as the routing metric to build multi-hop networks. ETX is used to convert number of communications into a link metric, which measures the quality of communication between nodes. This metric measures the relative distance to the root node via adjacent nodes to determine the parent node. However, this method of determining link metrics may cause nodes to frequently change their parents. If a node selects a parent with poor link quality, the communication reliability deteriorates; therefore, each node must appropriately select a candidate parent node. This paper presents the transmission characteristics of Wi-SUN FANs and highlights the problems of conventional link metrics. Based on this, a novel method is proposed for calculating the link metric. The performed computer simulations verified the superiority of the proposed metric when the packet generation rate remained unaffected by the generation of control frames that switched the parent nodes. Furthermore, the transmission success rate of the media access control (MAC) frame was experimentally measured in an office building using Wi-SUN FAN communication modules based on the proposed method. The evaluation confirmed that the proposed link metric improved the minimum MAC frame transmission success rate by 24.2% and the average success rate by 10.4%.

***Index Terms*—Expected transmission count, IEEE 802.15.4, IPv6 Routing Protocol Low-Power and Lossy Network, received signal level, Wireless Smart Utility Network Field Area Network**

I. Introduction[1]

THE Internet of Things (IoT) enriches society by collecting parameters from sensors and meters of various devices via wireless networks; the collected data are used to improve services and generate new applications [1][2]. The future of IoT is expected to include the installation of measurement instruments, such as sensors, meters, and monitors equipped with numerous wireless devices, over a wide area for data collection. Therefore, a wireless communication technology that can satisfy various demands according to usage models, such as low power consumption, extended communication distance, high transmission success rate, low manufacturing cost, smaller devices, and low latency, is essential.

Smart utility network (SUN) is one of the wireless communication standards for IoT based on the IEEE 802.15.4 international standard for personal area network (PAN) [3]; it is characterized by low power consumption, low cost, and low data rate communication performance [2][3]. SUN uses a frequency band below 1 GHz, referred to as Sub-1 GHz in the physical layer, which enables long-distance transmission ranging from several hundred meters to several kilometers with a power of approximately 20 mW [4]. Furthermore, carrier-sense multiple access with collision avoidance (CSMA/CA) is used in the media access control (MAC) layer to avoid radio wave interference between terminals and improve transmission efficiency. Wireless smart utility network (Wi-SUN), based on the physical and MAC layers that are compliant with IEEE 802.15.4 SUN, adds communication and authentication methods to the upper layer to realize various IoT applications. The technical

This work was supported by National Institute of Information and Communications Technology (NICT) in Japan (No. JPJ012368C05101) and the Ministry of Internal Affairs and Communications (MIC) in Japan (SCOPE No. JP196000002).

R. Nagao is with the Graduate School of Informatics, Kyoto University, Kyoto 606-8501, Japan (e-mail: nagao@dco.cce.i.kyoto-u.ac.jp).

D. Hotta is with the Graduate School of Informatics, Kyoto University, Kyoto 606-8501, Japan (e-mail: hotta@dco.cce.i.kyoto-u.ac.jp).

H. Masaki is with the Graduate School of Informatics, Kyoto University, Kyoto 606-8501, Japan (e-mail: hiroko.masaki@i.kyoto-u.ac.jp).

K. Mizutani is with the Graduate School of Informatics, Kyoto University, Kyoto 606-8501, Japan (e-mail: mizutani@i.kyoto-u.ac.jp).

H. Harada is with the Graduate School of Informatics, Kyoto University, Kyoto 606-8501, Japan (e-mail: hiroshi.harada@i.kyoto-u.ac.jp).

specifications and interoperability test specifications of Wi-SUN are determined by Wi-SUN Alliance, and multiple profiles have been established for various IoT applications [2]. Among them, the Wi-SUN for field area network (Wi-SUN FAN) [5]–[8] connects various measurement devices installed indoors and outdoors in a mesh-like configuration using multi-hop routing, necessary for building social infrastructure, such as smart meters and smart cities. Fig. 1 shows the basic configuration of Wi-SUN FAN. The Wi-SUN FAN, which is a PAN, constructs a destination-oriented directed acyclic graph (DODAG) using three types of nodes: border router (BR), router, and leaf. BR is the root node of a DODAG and access to wide area network (WAN). A router can have a parent node and child nodes, and it generates and forwards packets. A leaf is a terminal node without a child node and has minimal functionality, such as packet-generation, transmission, and reception [6]–[8].

In May 2016, Wi-SUN FAN was standardized by Wi-SUN Alliance as Wi-SUN FAN 1.0 for technical communication specifications [7], and Wi-SUN FAN 1.0 was further standardized as IEEE 2857 in June 2021 [6][8]. Hereafter, we refer to Wi-SUN FAN 1.0 as Wi-SUN FAN, which defines layers 1 to 4 of the Open Systems Interconnection (OSI) reference model [6]. The Sub-1 GHz frequency band was used in the physical layer, and SUN frequency shift keying (FSK) with data rates of 50, 100, and 150 kbps standardized in IEEE 802.15.4-2015 was adopted. In addition to CSMA/CA standardized in IEEE 802.15.4-2015, frequency hopping (FH), a technology that prevents interference by switching the band used by each node at specific intervals, was adopted in the MAC layer [6]–[8]. In the network layer, the Internet Protocol Version 6 (IPv6) Routing Protocol for Low-Power and Lossy Network (RPL), a routing protocol that enables multi-hop communication compatible with IPv6 communication, was adopted [9]. This enables multi-hop routing in more than 20 stages [6][7], and data collection from remote devices to the BR by using other wireless devices as routers. Even when direct communication with the BR is not possible, the blind zones can be reduced via multi-hop. Since May 2016, various studies on Wi-SUN FAN have been conducted based on its technical specifications [10]–[13]. Some parts of the Wi-SUN FAN system are to be introduced by users into the radio integrated circuit (IC) as a mandatory standard, and some parts can be freely changed by vendors to compete the transmission characteristics. Currently, Wi-SUN FAN is mostly used for fixed SUN, such as smart meter and other applications, and various parameters are set for these applications. However, other applications using multi-hop are also increasing. Therefore, the determination of vendor-dependent, changeable parameters for such purposes is needed. In this study, we focused on one of these changeable parameters related to RPL. In this study, we focused on reliable and high-speed methods for building Wi-SUN FAN multi-hop networks; we developed efficient methods for changing the connected node when the communication quality between nodes deteriorates after a multi-hop network.

The findings of this study are expected to increase the number of vendor-dependent items in Wi-SUN FAN. In addition, new standardization corresponding to new applications are expected to be started. Furthermore, this paper can also be used as a starting point for research and development to improve the transmission characteristics of new multi-hop networks.

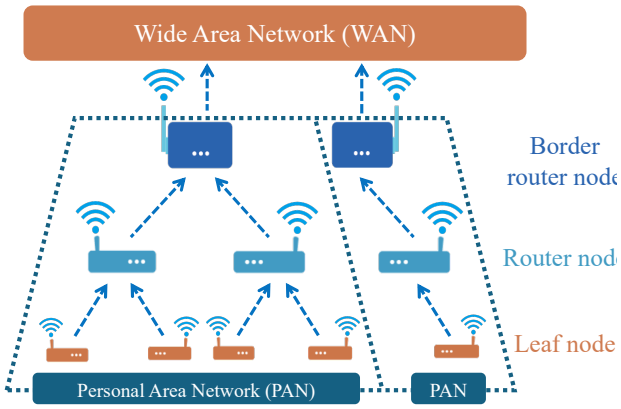

Fig. 1. Basic configuration of Wi-SUN FAN.

In RPL—the routing protocol adopted in Wi-SUN FAN—the rank is defined as an indicator of the relative distance from the BR to each node in the DODAG (Fig. 1) using control messages between nodes. To avoid network loops and construct an appropriate DODAG, nodes that are closer to the BR than themselves are autonomously selected as parent nodes. This process is repeated to build a very large multi-hop network. In Wi-SUN FAN, a method for selecting parent nodes based on minimum rank with hysteresis objective function (MRHOF) [14] is defined.

In the MRHOF, each node uses an index called link metric to determine and select a parent node to connect to. As link metrics, Wi-SUN FAN primarily uses: 1) the exponentially weighted moving average (EWMA) of the received signal level (RSL) for routing, which is a measure of received power, and 2) the EWMA of the expected transmission count (ETX), which is a measure of communication success rate [6]–[8]. The RPL using MRHOF with ETX is suitable for selecting links with higher communication quality than routing with hop count as the link metric. However, the parent node is frequently changed owing to biases in link quality estimation [15]. Moreover, nodes often select low-quality links during parental changes, which deteriorates communication reliability [16]. However, these evaluations correspond to RPL without Wi-SUN FAN, and whether the same problems are observed in Wi-SUN FAN is unclear. If this is the case, new link metrics and other methods are required to improve the transmission characteristics; however, no such proposal has been made thus far. In this study, the following three features were considered to develop a stable and reliable Wi-SUN FAN.

- We evaluated the packet transmission success rate and transmission delay characteristics of Wi-SUN FAN based on the link metric MRHOF, which uses RPL defined in Wi-SUN FAN 1.0, by computer simulation. We determined that when the transmission characteristics deteriorate owing to the existing parent node, the change in node requires time, leading to the deterioration of overall transmission characteristics.

- We developed a novel link metric that updates the routing to the appropriate parent when the communication reliability with the existing parent node is low.
- The effectiveness and feasibility of the proposed method was verified by evaluating: 1) the packet transmission success rate and packet transmission delay characteristics using computer simulations and 2) the MAC frame transmission success rate using Wi-SUN FAN devices.

Many scholars attempted to develop reliable methods of configuring multi-hop networks for Wi-SUN FAN. For example, Junjalearnvong et al. [10] developed a method to reduce construction time by optimizing the frequency of generating frames joining the network. Mizutani et al. [11] compared the performances of packet transmission success rates for different protocols between Wi-SUN FAN and time-synchronized channel hopping in FH. Furthermore, Hirakawa et al. [12] reported improvement in the packet transmission success rate by limiting the number of child nodes connected to each node in the RPL of the SUN FAN network layer. Lee and Chung [13] proposed a scheduling method to reduce latency while maintaining the unicast-to-broadcast throughput ratio in Wi-SUN FAN. However, to the best of our knowledge, no researcher has attempted to improve the transmission characteristics using a link metric, and multi-hop communication that involves RPL has not been experimentally evaluated using both computer simulations and actual equipment using the Wi-SUN FAN protocol stack. Therefore, the findings of this study can effectively contribute to the efficient implementation of Wi-SUN FANs for smart city infrastructure.

The remainder of this paper is organized as follows. The specification of Wi-SUN FAN are described in Section II. In Section III, the fundamental transmission characteristics of a Wi-SUN FAN multi-hop network with RPL are analyzed via computer simulations in terms of packet transmission success rate and transmission delay time. Additionally, the factors contributing to the degradation of the transmission characteristics are discussed. In Section IV, the proposed link metric that updates the destination to the appropriate parent node when communication with the existing parent node becomes unstable is described. The improvement in transmission characteristics and their evaluation with respect to a multi-hop routing scheme using the proposed link metric are discussed based on computer simulations. In Section V, the verification of the effectiveness of the proposed scheme using actual equipment is discussed. Finally, the study is concluded in Section VI .

II. Wi-SUN FAN

A. Protocol Stack

Fig. 2 depicts the protocol stack of Wi-SUN FAN, which defines layers 1–4 of the OSI reference model; details of each layer are described in [6]. Wi-SUN FAN uses various methods, such as CSMA/CA and FH, to prevent interference between each wireless device [6]. Herein, these wireless devices are referred to as nodes.

OSI Layer	Wi-SUN FAN Protocols
4: Transport	UDP/TCP
3 : Network	IPv6/ICMPv6/RPL/ 6LoWPAN
2 : Data Link	LLC Sub-Layer
	MAC Sub-Layer
1 : PHY	Physical Layer

Fig. 2. Protocol stack of the Wireless Smart Utility Network Field Area Network (Wi-SUN FAN).

B. FH

During FH, each node receives a frequency channel corresponding to an individually assigned channel schedule. Wi-SUN FAN employs two transmission modes for channel scheduling, namely, unicast and broadcast schedules [6]–[8]. Unicast schedules are generated based on the MAC address of a node and differ for each node. The unicast schedule specifies a receiving channel for each time interval, referred to as the unicast dwell interval (UDI). Furthermore, as unicast schedules are shared among the nodes, each node can understand the unicast schedules of its adjacent nodes.

Broadcast schedules are generated based on a value unique to the PAN, referred to as the broadcast schedule identifier (BSI). BSI is advertised to all nodes in the PAN and is common among the nodes belonging to that PAN. Furthermore, the common channel defined in the broadcast schedule is used by all nodes. Both the broadcast and unicast switches are operated at regular intervals, with a duration of one cycle defined by the broadcast interval (BI). The broadcast schedule updates the receiving channel for each cycle, and the time interval during which broadcasts are performed is defined as the broadcast dwell interval (BDI). Each node prioritizes receiving the channel specified in the broadcast schedule over a unicast schedule. However, the unicast schedule is prioritized over the broadcast schedule in the time durations outside BDI.

C. RPL

1) Network Model

In RPL, as shown in Fig. 1, the BR collects data from the nodes in the PAN and transmits the collected data to the WAN. The router can have a parent and child nodes in addition to BR, whereas a leaf does not have child nodes. Each node calculates the link and routing metrics using a certain method and determines the parent node to be connected using the calculation results of these metrics. Each node transmits a predefined control frame to BR through the determined parent node. The BR returns a receipt notice regarding each parent node determined by each node. Subsequently, a routing table is constructed to transmit information from BR to each router and leaf. Each node completes route construction by receiving a receipt notice from BR.

2) Control Frame

RPL uses the following four control frames to form the topology [6]–[9].

- DODAG Information Solicitation (DIS): This frame is broadcast at regular intervals to request a DODAG Information Object (DIO) frame from a node not connected to the network.
- DIO: This frame is broadcast at intervals determined by a trickle timer [17] used to select a parent and maintain the routing table. The node that receives the DIS frame shortens its transmission interval.
- Destination Advertisement Object (DAO): A frame unicasts a node's own parent information to BR at regular intervals. This frame is transmitted after a certain period has elapsed or when a node changes its parent node.
- DAO Acknowledgement (DAO-ACK): An acknowledgement frame that confirms the receipt of the DAO frame when BR receives it. The BR transmits this unicast frame to the node from which DAO is sent.

3) Link Metric and Routing Metric

A routing metric is used to evaluate and optimize the path from each node to BR. As explained in Section I, Wi-SUN FAN employs MRHOF [6], [13] that uses EWMA of RSL and ETX for parent selection. If the values of RSL and ETX are in a particular time series, X (t = 0,1,2...), then each EWMA can be defined as follows:

$$X_{\mathrm{EWMA}}(t) = \tilde{S} \cdot X(t) + \left(1 - \tilde{S}\right) \cdot X(t-1), \quad (1)$$

where $\tilde{S}$ denotes the smoothing factor. Its default value is set to 1⁄8 in Wi-SUN FAN [8].

In Wi-SUN FAN, EWMA of RSL is calculated in the range of 0 to 254 by adding a bias of 174 to the received power ranging from -174 dBm to +80 dBm. Every packet from which an ACK frame is returned is notified of the RSL value, and the EWMA is updated each time the RSL value is obtained.

ETX is a link metric that uses the success rate of communication between nodes and can be defined as

$$X_{\mathrm{ETX}} = 128 \cdot \frac{T}{S}, \quad (2)$$

where T denotes the number of transmission attempts, and S indicates the number of ACKs received. The maximum value of ETX is 1024, and the initial value of EWMA of ETX is 256. When over four frames have been transmitted and over 1 min has passed since the last update of the EWMA of ETX, ETX is recalculated, and the EWMA of ETX is updated. Based on the EWMA of ETX, each node calculates the path cost and rank as an index for route selection.

The path cost is used to evaluate the path to BR. Each node preferentially selects the path with the lowest path cost from the list of parent node candidates using MRHOF. In Wi-SUN FAN, the path cost can be calculated by summing the rank of a parent node candidate and its EWMA of ETX up to each parent node. The path cost from node N to its parent candidate κ can be obtained as

$$\vartheta_N(\kappa) = \min\{X_{\mathrm{EWMA}}(N,\kappa) + \varrho(\kappa),\ 32768\}, \quad (3)$$

where $X_{\mathrm{EWMA}}(N,\kappa)$ denotes the EWMA of ETX calculated based on the communication success rate of node N with its candidate parent κ, and $\varrho(\kappa)$ represents the rank of the parent candidate κ obtained from DIO.

The rank is a measure of the distance required to communicate with the BR in the PAN. As a node moves away from the BR, its rank increases because the number of multi-hops required to connect with it increases. In Wi-SUN FAN, the rank of a node N can be calculated using its parent node k, as follows:

$$\begin{cases} \varrho(N) = \hat{A}, & (N\text{: BR}) \\ \varrho(N) = \max\left[\min\{\varrho(k) + \hat{A}, 65535\}, \vartheta_N(k)\right] & (N\text{: Other}), \end{cases} \quad (4)$$

where $\hat{A}$ represents the minimum rank, which is 128 for Wi-SUN FAN 1.0.

D. Route Selection

RPL route construction using the MRHOF exhibits a hysteresis characteristic that prevents frequent route changes owing to minute changes in metrics.

1) Uplink Route Construction

Initially, a list of candidate parent nodes is prepared for each node; these parent nodes are neighboring nodes whose EWMA of RSL exceeds a specific threshold. This list of adjacent nodes is referred to as the parent candidate list. Operations such as adding or deleting the adjacent node ξ using node N from the parent candidate list are performed based on the following conditional expressions with hysteresis properties.

- Adding to the list of parent candidates:

$$X_{\mathrm{EWMA}}(N,\xi) > \hat{X} + \hat{Y} + \hat{Z}. \quad (5)$$

- Deleting from the list of parent candidates:

$$X_{\mathrm{EWMA}}(N,\xi) < \hat{X} + \hat{Y} - \hat{Z}, \quad (6)$$

where $X_{\mathrm{EWMA}}(N,\xi)$ represents the EWMA of RSL of the neighboring node ξ of node N, $\hat{X}$ denotes a vendor-dependent constant, $\hat{Y}$ indicates the threshold for adding the candidate parent list, and $\hat{Z}$ represents the hysteresis constant; in Wi-SUN FAN, $\hat{Y}$ = 10 and $\hat{Z}$ = 3.

Subsequently, each node calculates the path cost $\vartheta_N(\kappa)$ based on the rank information $\varrho(\kappa)$ obtained from DIO of the parent candidate node κ. Finally, the node selects a parent node with the minimum path cost $\vartheta_N(\kappa)$ from the list of parent candidates. The information of the selected parent node is conveyed to BR using DAO via unicast. When the path costs of the parent node or parent candidate nodes are updated or a new parent candidate node is added, a node reselects its parent node. Even if a parent candidate node κ exists with a lower path cost than the current parent node, the node maintains the connection with the current parent if the

difference between the path cost of the current and new parents is less than a threshold of $\hat{T}$.

2) Downlink Route Construction

To establish the downlink route, each node transmits a neighbor solicitation (NS) to BR and registers its IPv6 address with the parent node. The BR specifies the downlink route using the routing table and returns DAO-ACK to the source node; the downlink route is completed when each node receives DAO-ACK. If DAO-ACK is not received within a certain period, the node retransmits DAO.

III. Fundamental Transmission Characteristics of Wi-SUN FAN

We used computer simulations to analyze the fundamental transmission characteristics of the multi-hop network constructed using RPL in Wi-SUN FAN in terms of transmission success rate and transmission delay time of packets. The factors influencing the degradation of transmission characteristics are also discussed.

A. System Model Used for Computer Simulations

In the system model used for the simulations, 100 routers were randomly placed in an area with length and width of 4000 m each. The height of each router was limited to 1–10 m. The BR was placed at a height of 3 m at the center of the area. A total of 10 configurations were used to evaluate the transmission characteristics. A packet transmission simulation was performed for each arrangement. Data packets were not generated for 500 s after initiating the simulation, and routing was performed using RPL. Fig. 3 illustrates an example of router arrangement. After 500 s, the transmission of the DAO frames, which were periodically transmitted every 60 s, was interrupted to avoid collisions with the data packets generated at each router; a total of 200 data packets were generated at fixed intervals. The generated packets were forwarded to BR along the path constructed by RPL. The transmission characteristics were evaluated for the 50th to 149th packets generated by each router. The parameters used in the simulations are listed in Table I.

B. Evaluation Index

In this study, we used the average transmission success rate and average transmission delay time of packets as evaluation indices. The transmission success rate denotes the ratio of the number of packets successfully received at BR to those originated at other nodes. The delay time represents the time elapsed between the origin of a packet and its successful reception at BR. We evaluated the average of the results for each of the 10 router configurations.

C. Simulation Results

The program for the computer simulation was developed using MATLAB_R2023b [6]. The transmission success rate characteristics and delay time of 100 Wi-SUN FAN nodes with this simulator have been compared and verified with experimental evaluation of actual devices in [6], wherein the simulation and experimental results were in good agreement.

The packet generation frequency λ can be defined as the reciprocal of the transmission interval time of each router;

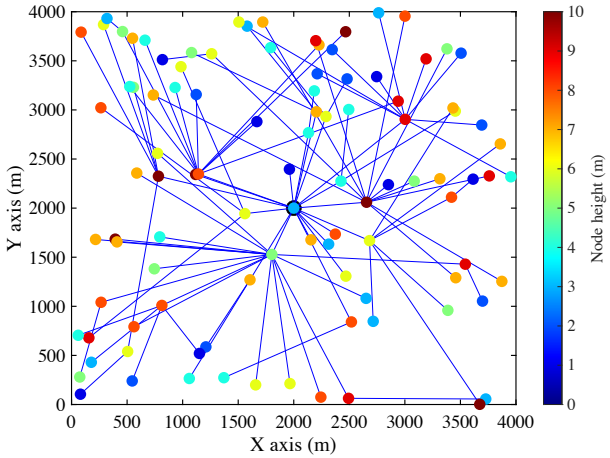

Fig. 3. Example of a router arrangement.

TABLE I
Parameters Used in The Simulation

Parameters	Values
Number of routers	100
Node height	1–10 m
Transmission power	13 dBm
Data rate	150 kbps
Packet length	340 bytes
Capture ratio	13 dBm
RSSI threshold	-90 dBm
Clear channel assessment (CCA) threshold	-84 dBm
Packet buffer size	14
Unicast dwell interval (UDI)	0.25 s
Broadcast interval (BI)	1 s
Broadcast dwell interval (BDI)	0.1 s
Number of FH channels	14
Minimum backoff exponent	4
Maximum backoff exponent	4
Maximum number of backoff	5
Maximum number of retransmissions	4
CCA duration	128 μs
Long inter-frame space (LIFS)	5.3 ms
ACK waiting duration	144 ms
ACK frame size	72 bytes
DIS sending interval	30 s
DIS packet length	84 bytes
DIO trickle timer $I_{\min}$	1.024 s
DIO trickle timer $I_{\max}$	7
DIO packet length	127 bytes
DAO sending interval	60 s
DAO packet length	145 bytes
Maximum number of DAO retransmissions	5
DAO retransmission interval	5 s
DAO-ACK packet length	115 bytes
Threshold of $\hat{T}$	96

Figs. 4 and 5 depict the transmission success rate and average delay time considering λ, respectively. Each router performs carrier sensing before transmitting a packet and does not transmit a packet if the bandwidth used for the transmission is occupied by another router. Therefore, the time required for transmission when the occupied bandwidth is used by another router increases with an increase in λ, thereby deteriorating the transmission characteristics. Additionally, when RPL is used for routing, one parent router may contain several child nodes, which transmit packets to BR via the parent router. When packets are transmitted from multiple

This article has been accepted for publication in IEEE Open Journal of Vehicular Technology. This is the author's version which has not been fully edited and content may change prior to final publication. Citation information: DOI 10.1109/OJVT.2025.3534842

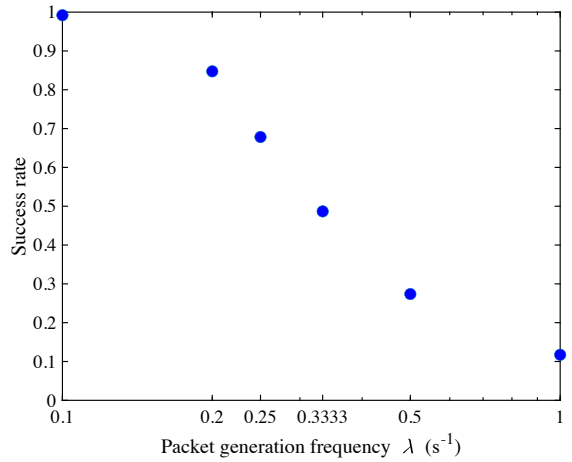

Fig. 4. Average transmission success rate of conventional methods.

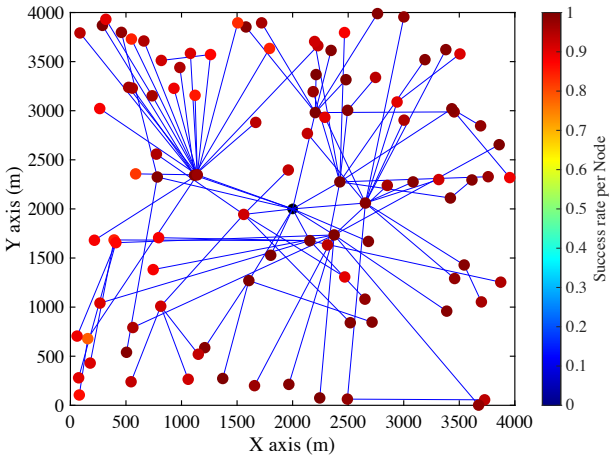

Fig. 6. Transmission success rate per router at $\lambda = 0.2$.

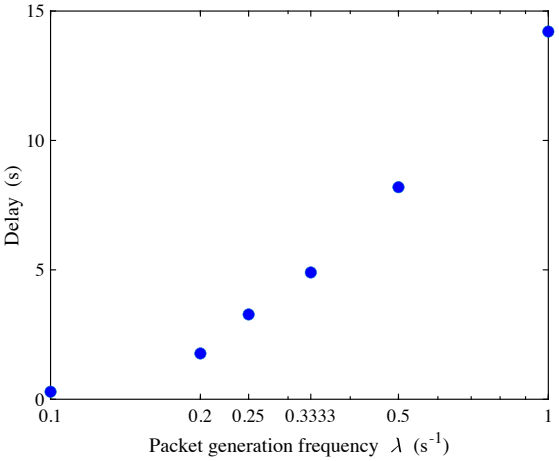

Fig. 5. Average transmission delay time in the conventional method.

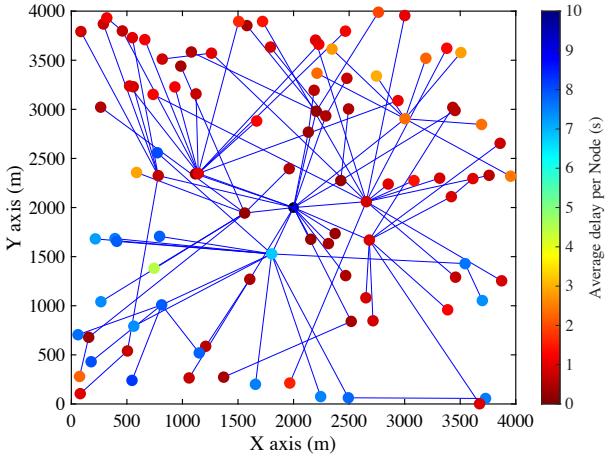

Fig. 7. Average transmission delay time per router at $\lambda = 0.2$.

child nodes at a high frequency, they are temporarily stored in the transmission buffer of the parent node and sequentially forwarded to BR. Therefore, packets tend to accumulate in the buffer as λ increases, thereby increasing the transmission delay, which is the period from packet generation to reception at BR.

Figs. 6 and 7 illustrate the result of the transmission success rate and transmission delay time for each router at $\lambda = 0.2$, respectively. The average transmission success rate and average delay time were 0.8528 and 1.6656 s, respectively; however, the transmission characteristics were divided into two groups depending on the position of the router. Several routers on the lower side of BR exhibited a transmission success rate of less than half, and the delay time in most of these routers was approximately 10 s. Most of these routers selected the router located at (1803 m,1528 m) as the parent node, and several packets were discarded at this router. However, the link metric (Section II) did not update the route to BR as long as communication with the parent node was successful. Therefore, the transmission characteristics did not improved. This indicates that an improved link metric that can instantly reroute when the reduction in communication success rate is essential to construct a highly reliable network.

IV. Multi-hop Routing Scheme Based on the Proposed Link Metric

As established previously, the link metrics that do not change the parent node despite the deterioration in transmission characteristics are one of the factors affecting the deterioration of transmission characteristics owing to the increased frequency of packet generation. To address this problem, we proposed a novel link metric that updates the destination to the appropriate parent node when communication with the existing parent node is unreliable. We evaluated the transmission characteristics of a multi-hop routing scheme using the proposed link metric by computer simulations. We compared the simulation results with those obtained from the conventional multi-hop routing scheme (Section III).

A. Proposed Link Metric

In the conventional Wi-SUN FAN, the link metric, ETX, is calculated using (2). By contrast, the proposed link metric can be represented by replacing (2) as follows:

$$\begin{cases} X_{\mathrm{ETX}} = \dfrac{128}{\varpi} & (\varpi > \psi) \\ X_{\mathrm{ETX}} = \min\left(\dfrac{128}{\psi}\log_{\psi}\varpi, 1024\right) & (\varpi \le \psi) \end{cases}. \tag{7}$$

In case of (2) or (7), the maximum value of ETX is 1024 and limited to a maximum of 10-bit integer values; the ETX are calculated with fractions rounded down. Therefore, using (7) instead of (2) does not change the complexity of the calculator. The proposed link metric defines a target transmission success rate, referred to as the threshold (ψ). If the success rate of MAC frames (ϖ) $> \psi$, ETX can be calculated using (2), whereas the newly proposed formula is applied if $\varpi \leq \psi$. The initial value of the link metric is 256, which corresponds to $\varpi = 0.5$.

In (2), the ETX increase ratio depends on $1/\varpi$ when the communication success rate at the MAC layer decreases. However, ETX does not increase much when the communication quality degrades with an increase ratio of $1/\varpi$, and router change remains difficult. Therefore, to encourage route changes, we used an increase ratio of $1/\log\varpi$, which has a steeper gradient than $1/\varpi$, in the proposed method. However, simply changing the equation to 128/logϖ would cause the ETX to rise unnecessarily even in places where it is not necessary to rise above the threshold ψ. To avoid this issue, in (7), the original equation shown in (2) is used when $\varpi > \psi$ and the new equation based on 128/logϖ is used when $\varpi \leq \psi$ to calculate ETX.

Fig. 8 depicts the relationship between the transmission success rate ϖ of the MAC frame and the link metric X_{ETX} at ψ = 0.8. The blue and red dotted lines represent the conventional and proposed link metrics, respectively. The figure further indicates the initial value of the link metric, which is 160 for ψ = 0.8 in the proposed method. When the transmission success rate of MAC frames (ϖ) was lower than ψ, the link metric of the proposed method increased significantly, which stimulated the switching of the parent node. This can aid in maintaining the transmission success rate of each router around ψ as it enables the selection of another router as the parent node whenever the success rate of MAC frames (ϖ) $\leq \psi$.

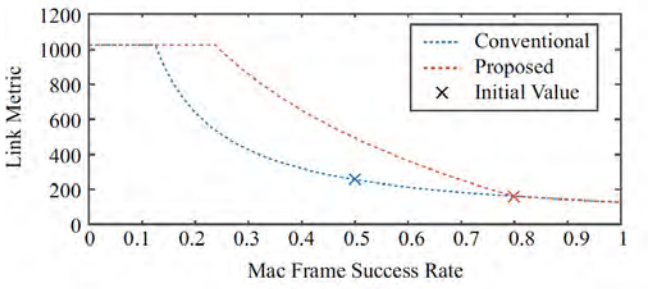

Fig. 8. Relationship between the media access control (MAC) frame communication success rate and link metrics.

B. System Model and Evaluation Index

The system model described in this section uses the same parameters and router configurations as those presented in Section III. Here, the target transmission success rate threshold ψ was set to 0.95, 0.90, 0.85, 0.80, 0.75, and 0.70, and simulations were performed for each of these six values. The same average transmission success rate and average transmission delay time as those presented in Section III were used as the evaluation indices; the results were compared with those obtained using the conventional method.

C. Computer Simulation Results

Fig. 9 illustrates the transmission success rate for λ in computer simulations with the proposed metric; the conventional method described in Section III is indicated in blue.

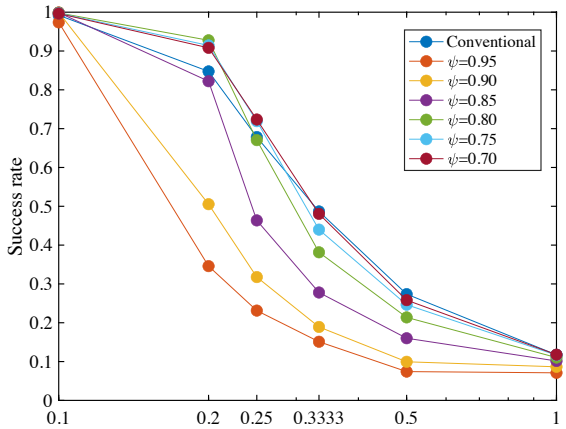

Fig. 9. Average transmission success rate using the proposed method.

For $\psi \geq$0.90, the transmission characteristics deteriorated more significantly than those observed in the conventional method. Although ψ was set as a threshold for the transmission success rate of MAC frames, it denoted communication failures caused not only by packet collisions but also by repetitive backoff when the destination router was communicating with another router. Therefore, the transmission success rate of MAC frames decreased for most routers as λ increased, resulting in switching of the parent node. When the parent node was switched, a DAO frame (control frame) was forwarded to BR during route update; however, this frame was transmitted at the same time as the packet, overloading the network and thereby significantly reducing the transmission efficiency.

The conventional method exhibited the best transmission characteristics for $\lambda \geq$ 0.33. The network load increased with the increase in packet generation rate, and the transmission success rate of MAC frames reduced below ψ regardless of the router selected by the parent candidate. Therefore, a router different than the currently selected parent node was selected for every update in the link metric, generating a control frame each time. Consequently, the transmission characteristics were not better than those of the conventional method. In general, when a node changes its transmission route, it sends a DAO frame to convey the changed routing information to the BR. Then, the BR determines the changed route by responding to the node with a DAO-ACK frame. However, the sending and receiving of these control frames is different from data packets. Therefore, we did not include them in the transmission success rate when evaluating the transmission characteristics. When a

This article has been accepted for publication in IEEE Open Journal of Vehicular Technology. This is the author's version which has not been fully edited and content may change prior to final publication. Citation information: DOI 10.1109/OJVT.2025.3534842

node changes its transmission route, this series of processes is mixed with the transmission of data packets. Therefore, the communication load increased, and the transmission characteristics deteriorated.

However, for $\lambda \leq 0.25$, the amount of improvement in transmission characteristics when the parent node was switched exceeded the load on the network caused by the control frames transmitted on the switching; consequently, the overall transmission characteristics were improved. At λ = 0.2, the packet transmission success rate of the conventional method was 84.7%, whereas the proposed method at ψ = 0.8 exhibited a success rate of 92.7%, which is an increase of 8.0%.

Fig. 10 depicts the delay between the transmission of a packet and its reception by a BR. For $\lambda \geq 0.5$, the conventional method exhibited the longest average delay time. Typically, packets that require multiple hops to reach BR tend to fail to be transmitted when the transmission efficiency deteriorates. However, the average transmission time in the proposed scheme was shorter than that of the conventional method. This is because packets with a relatively small number of hops accounted for the majority of successfully transmitted packets.

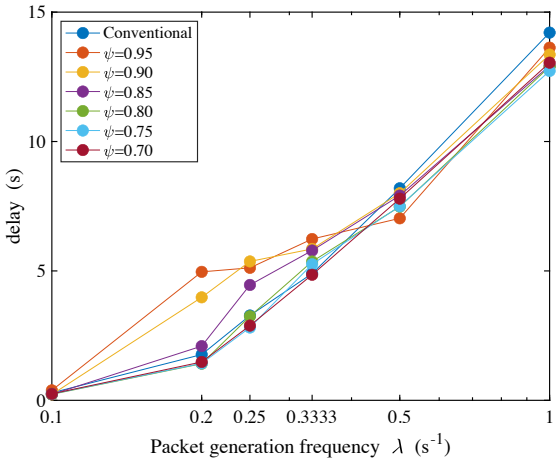

Fig. 10. Average delay using the proposed method.

For $\lambda \leq 0.25$, the average delay time was shorter than that of the conventional method for $\psi \leq 0.8$. Although DAO frames were transmitted more frequently in the proposed method than in the conventional method and the delay time was increased, the reduction in transmission delay outweighed the disadvantages induced by DAO frames. This is because the route to BR was reconstructed by updating the network.

Fig. 11 depicts the transmission success rate per router using the proposed method with λ = 0.2 and ψ = 0.8 following the router arrangement presented in Fig. 3. While the transmission characteristics were bifurcated in the conventional method, the router at the end maintained high transmission characteristics. The transmission characteristics were not degraded below ψ because in the proposed method, the parent node was switched each time the transmission success rate reduced below ψ. Although switching the parent node generates new control frames, the number of control packets generated may not be high enough to affect the data packets. Therefore, high transmission performance was achieved even at the final node of the network.

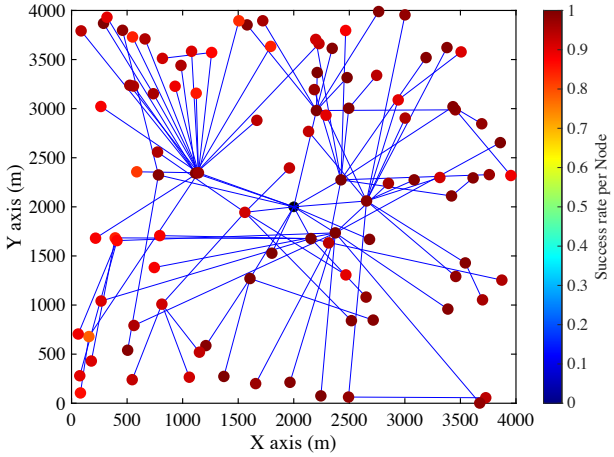

Fig. 11. Transmission success rate per router using the proposed method at λ = 0.2 and $\boldsymbol{\psi}$ = 0.8.

V. Evaluation Using Actual Equipment

The simulations explained in Section IV confirmed the superiority of the proposed link metric over the conventional method in terms of the frequency of packet generation when control frames did not affect data packets. In this section, the characteristic verification of the proposed method, performed by applying it in an actual machine environment, are discussed.

A. Experimental Equipment Configuration

Fig. 12 depicts the IoT terminal with the Wi-SUN FAN module used in the experiment. The IoT terminal was equipped with Wi-SUN module BP35C5 (ROHM Semiconductor) on an adapter board. The Wi-SUN module, equipped with Wi-SUN FAN-compatible firmware, was controlled via serial communication. The IoT terminal was powered by a Windows PC via USB cable (Fig. 13); the PC was responsible for restarting the Wi-SUN module, generating data packets, and acquiring experimental data logs.

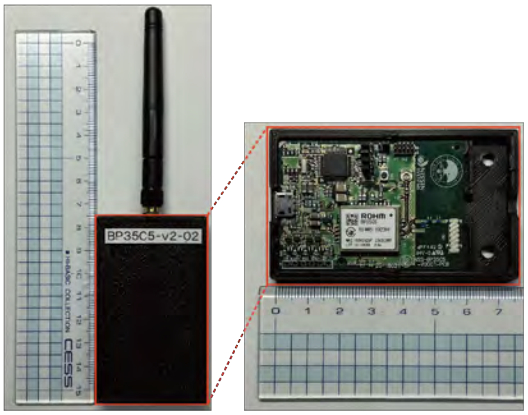

Fig. 12. IoT terminal with the Wi-SUN FAN module.

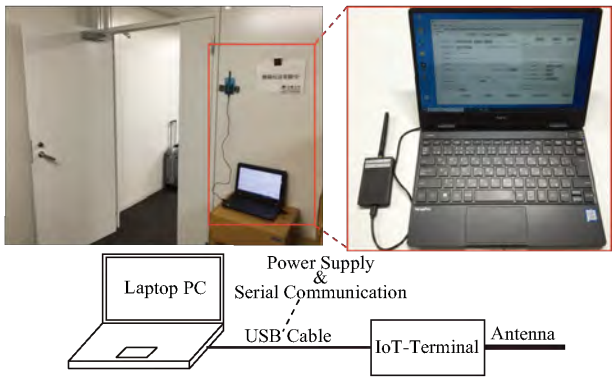

Fig. 13. Configuration of the experimental equipment.

B. Experimental Environment

The experiment was conducted in the West Wing of the International Science Innovation Building on the Yoshida Campus of Kyoto University. We installed one BR and 12 routers in the corridors and living rooms on the second floor, corridors on the third floor, corridors on the fourth floor, and at the stairs from the second to fourth floors (Fig. 14).

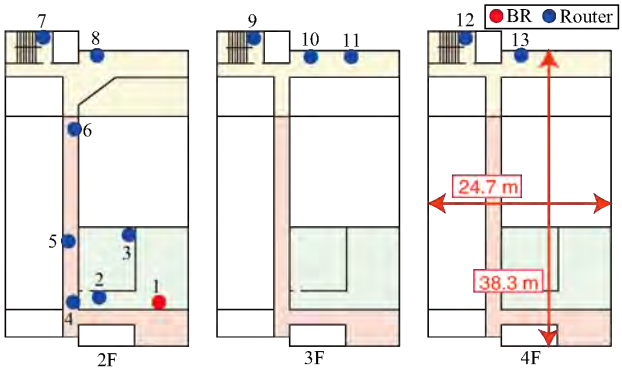

@Kyoto University, International Science Innovation Building (West Wing)

Fig. 14. Experimental environment.

Hereafter, each router is referred to by the number presented in Fig. 14; for instance, router 2 is referred to as R2. The height of each terminal from the floor was 0.95 m for BR; 1.65 m for R2–R6 and R8; 1.1 m for R7, R9, and R12; and 0.5 m for R10, R11, and R13. The experiment was performed using the following procedure. All terminals were simultaneously powered on after setting up the router. No packets were generated for 30 min, and only control frames were transmitted at regular intervals to build the network. Subsequently, 350 packets were generated from R2 to R13 at regular intervals with $\lambda = 0.2$ to investigate the transmission characteristics. The experiment was repeated 10 times for the conventional and proposed methods, each, by varying the link metric, and the transmission success rates of the MAC frames were compared. We evaluated the proposed method with $\psi = 0.8$, because $\psi \geq 0.9$ was likely to significantly degrade the transmission characteristics (Fig. 9). The parameters used in the experiment are listed in Table II.

TABLE II
PARAMETERS USED IN THE EXPERIMENT

Parameters	Values
Number of routers	12
Transmission power	13 dBm
Data rate	150 kbps
Packet length	128 bytes
Packet transmission interval	5 s
RSSI threshold	−96 dBm
CCA threshold	−84 dBm
Number of FH channels	1
DIS sending interval	30 s
DAO sending interval	60 s
Modulation scheme	2-GFSK
Antenna gain	2.15 dBi
Threshold of $\hat{T}$	96

C. Evaluation Results of Transmission Characteristics

Fig. 15 depicts the transmission success rates of the MAC frames for each router obtained from the 10 experiments. The characteristics of the proposed and conventional methods are indicated in blue and red, respectively. The average transmission success rates for R3, R9, R13, and all nodes with 10 trials are illustrated in Fig. 15(a), and Fig. 15(b) presents the minimum values.

As shown in Fig. 15(a), almost no change occurred in the average transmission success rate of MAC frames for R3; however, improvement was observed for R9 and R13 when the proposed method was used. This is because R3 could directly communicate with BR from its router location and was less susceptible to route construction; conversely, R9 and R13, which were farther from BR, were optimized using the proposed method to select appropriate parent nodes. The improvement was more remarkable in the lowest success rate of MAC frame communication (Fig. 15(b)); the lowest rate of 65.2% was observed in R9 with the conventional method; conversely, an improvement of 24.2% (from 65.2% to 89.4%) was observed with the proposed method. Additionally, the minimum success rate of MAC frame

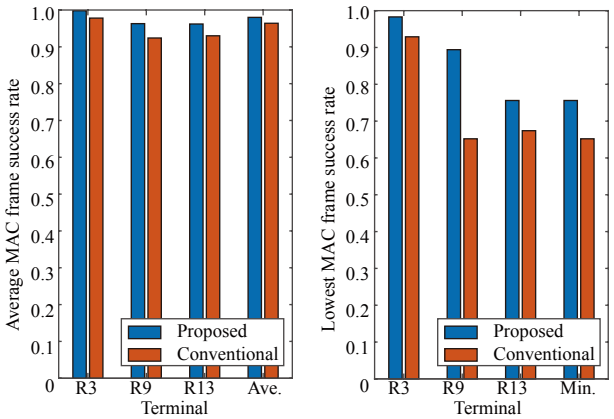

(a) Average MAC frame success rate in all trials

(b) Lowest MAC frame success rate in all trials

Fig. 15. Average transmission success rate of the MAC frames for each router obtained in the actual experiment.

communication for all nodes improved by 10.4% (from 65.2% to 75.6%). This is because when the transmission success rate of MAC frames reduced below $\psi = 0.8$, the link metric in the proposed method was larger than that in the conventional method (Fig. 8). This facilitated the change in the parent node when the rate was substantially lower than ψ. Therefore, the transmission success rate of MAC frames did not reduce significantly below ψ when the proposed method was employed.

Next, we focused on router R9 and compared the two methods with respect to the time variation of the link metrics at the selected parent. According to the router layout depicted in Fig. 14, the three candidate parents for R9 included R6, R7, and R8. However, the route between the routers was large when communicating between R6 and R8 and included several obstacles. Therefore, the communication success rate was not expected to be high. However, a high communication success rate was expected when communicating with R7 because the two routers were positioned above and below each other and were not far apart. Therefore, we assumed that R6 and R7 were the parents with low and high communication reliability, respectively.

Initially, we focused on the behavior when R9 selected a parent node, which was an unreliable communication when the conventional method was implemented. Fig. 16 depicts the variation in the transmission success rate obtained using the conventional method when R9 established communication with the selected parent R6. Fig. 17 illustrates the variation in the link metric (X_{ETX}) in the selected parent R6 when communicating with R9. As indicated in Fig. 16, the transmission success rate of the MAC frames remained low, with an average of 0.673. The initial value of the link metric when selecting a parent for the first time for all nodes in the network was 256, corresponding to a transmission success rate of 0.5. The link metric was gradually updated to a smaller value if the success rate was greater than 0.5. Therefore, the link metric (Fig. 17) approached 190, corresponding to an average success rate of 0.673. However, the fluctuation in the link metric was small in the conventional method even when the success rate was low. The link metric of the parent candidates other than R6 was as large as 256, corresponding to a success rate of 0.5; therefore, the parent node was not switched, leading to the selection of the parent node with the lowest success rate.

Subsequently, we focused on the behavior when R9 selected a parent with low communication reliability using the proposed method. Fig. 18 depicts the change in the communication success rate between R9 and the selected parents R6 and R7 by the proposed method. Fig. 19 illustrates the change in the link metric for the selected parents of R9, namely, R6 and R7. The success rate of R9 (Fig. 18) remained low at an average of 0.671 until approximately 1700 s when R6 was selected as the parent; however, the value reached 1.0 when the parent was changed to R7. This was because the path cost difference between R6 and R7 exceeded the threshold for the parent change $\hat{T}$. Typically, the path cost is calculated as the sum of the ranks of the parent candidate node and link metric. If their ranks do not significantly differ, the parent is selected based on the

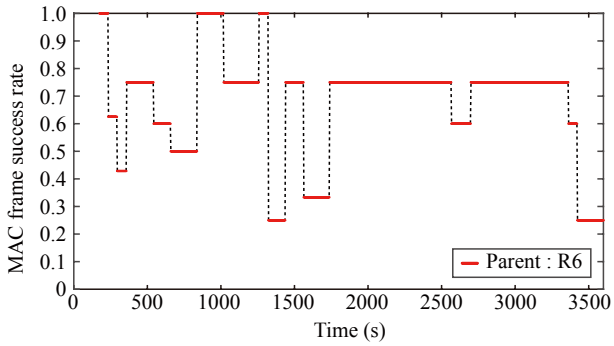

Fig. 16. Variation in the MAC frame communication success rate when R9 communicates with the selected parent R6 using the conventional method.

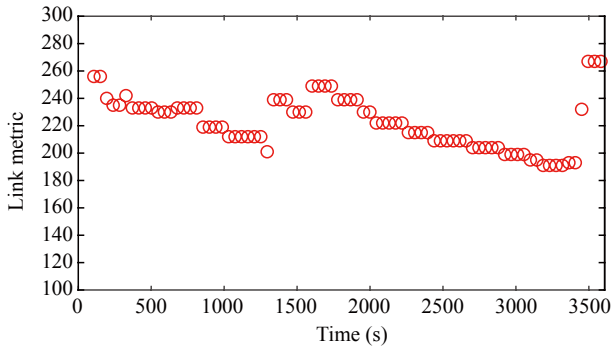

Fig. 17. Link metric variation when R9 communicates with the selected parent R6 using the conventional method.

link metric value. Therefore, in this experiment, the parent node was changed from R6 to R7. The amount of change in the link metric increased in the case of the proposed method when the transmission success rate of MAC frames (ϖ) $\leq \psi$, and the initial value of the link metric was 160; this corresponded to the parent change threshold ψ, smaller than that observed in the conventional method. Therefore, the variation in the path cost increased, and R9 identified a parent candidate node whose path cost was less than $\hat{T}$. Consequently, the parent was changed from R6 to R7 with a higher communication quality, thereby improving the transmission success rate of the MAC frames (Fig. 15).

We concluded that the proposed link metric improved the average success rate. This is because when routers far from BR (e.g., R9 and R13) connected to an unreliable parent node,

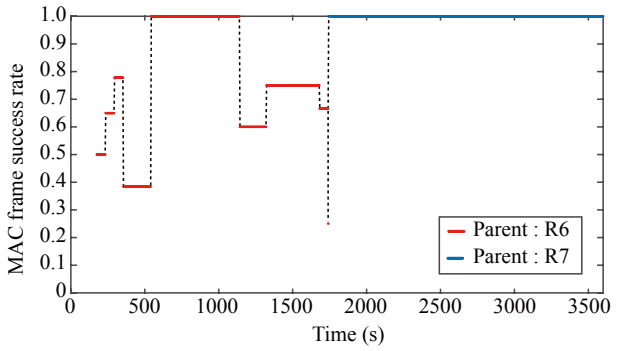

Fig. 18. Variation in the MAC frame communication success rate when R9 communicates with the selected parent R6 using the proposed method.

they appropriately switched to a reliable parent candidate node. If R6 with low reliability was selected as the parent for R9 in the conventional method, then the parent node would not have changed. However, the proposed method changed to a parent node with high reliability. Therefore, the proposed link metric can improve communication reliability.

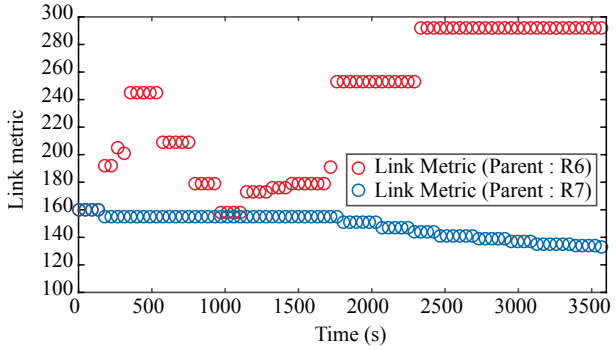

Fig. 19. Link metric variation when R9 communicates with the selected parent R6 using the proposed method.

VI. Conclusion

In this study, we analyzed the transmission characteristics of Wi-SUN FAN and examined the problems associated with conventional link metrics to develop a novel link metric calculation method. We performed simulations considering a scenario where the packet generation frequency was not affected by the control frame that switched the parent node. We determined that the proposed method was superior to the conventional method in terms of both transmission success rate and transmission delay time of packets. Furthermore, the simulation results indicated that the proposed method improved the transmission success rate of packet by 8.0% compared with the conventional method. A similar scenario was experimentally investigated using an actual machine. When the proposed method was implemented, the router connected to an unreliable parent appropriately switched the connection to a reliable parent candidate node, improving the minimum transmission success rate of MAC frames per node by up to 24.2%, with an average of 10.4%, compared with the conventional method. These findings confirm that the proposed method enables the construction of a stable and highly reliable Wi-SUN FAN, which can be used in a wide range of fields for IoT wireless communication infrastructure.

References

[1] U. Raza, P. Kulkarni and M. Sooriyabandara, "Low Power Wide Area Networks: An Overview," in *IEEE Communications Surveys & Tutorials*, vol. 19, no. 2, pp. 855-873, Secondquarter 2017, doi: 10.1109/COMST.2017.2652320.

[2] H. Harada, K. Mizutani, J. Fujiwara, K. Mochizuki, K. Obata, and R. Okumura, "IEEE 802.15.4g Based Wi-SUN Communication Systems," *IEICE Trans. Commun.*, vol. E100-B, no. 7, pp. 1032–1043, Jul. 2017.

[3] *IEEE Standard for Low-Rate Wireless Networks*, IEEE Standard 802.15.4-2015, IEEE, NJ, USA, Apr. 2016.

[4] Y. Xiang, R. Okumura, K. Mizutani and H. Harada, "Data Rate Enhancement of FSK Transmission Scheme for IEEE 802.15.4-Based Field Area Network," in *IEEE Sensors Journal*, vol. 21, no. 7, pp. 9600-9611, 1 April1, 2021, doi: 10.1109/JSEN.2021.3053158.

[5] Wi-SUN alliance, "Wi-SUN Alliance," https://www.wi-sun.org

[6] R. Hirakawa, K. Mizutani, and H. Harada, "Specification and performance analysis of Wi-SUN FAN," *IEEE Open J. Veh. Technol.*, vol. 4, pp. 849–866, Oct. 2023.

[7] Wi-SUN Field Area Network Working Group (FANWG), "Technical Profile Specification Field Area Network," vol.1v00, May. 2016.

[8] *IEEE Standard for Wireless Smart Utility Network Field Area Network (FAN)*, IEEE Standard 2857-2021, IEEE, NJ, USA, Jun. 2021..

[9] T. Winter, P. Thubert, A. Brandt, J. Hui, R. Kelsey, P. Levis, K. Pister, R. Struik, JP. Vasseur, and R. Alexander, "RPL: IPv6 Routing Protocol for Low-Power and Lossy Networks," IETF RFC 6550, Mar. 2012.

[10] T. Junjalearnvong, R. Okumura, K. Mizutani., and H. Harada, "Performance evaluation of multi-hop network configuration for Wi-SUN FAN systems.", Proc. 2019 16th IEEE Annual Consumer Communications & Networking Conference (CCNC), pp. 1-6.

[11] K. Mizutani, R. Okumura, K. Mizutani, and H. Harada, "Coexistence of synchronous and asynchronous MAC protocols for wireless IoT systems in sub-gigaherz band," in Proc. WF-IoT, Jun. 2020, pp. 1–6.

[12] R. Hirakawa, R. Okumura, K. Mizutani, and H. Harada, "A Novel routing Method with Load-Balancing in Wi-SUN FAN Network," in Proc. WF-IoT 2021, June. 2021.

[13] H-J. Lee and S-H Chung, "A Scheduling Method for Reducing Latency in Wi-SUN FAN Networks" in 2023 Fourteenth International Conference on Ubiquitous and Future Networks (ICUFN), Aug. 2023.

[14] O. Gnawali and P. Levis, "The Minimum Rank with Hysteresis Objective Function," IETF RFC 6719, Sep. 2012

[15] O. Iova, F. Theoleyre, and T. Noel, "Stability and efficiency of RPL under realistic conditions in wireless sensor networks," in Proc. IEEE PIMRC, Sept. 2013, pp.2098-2102.

[16] E. Ancillotti, R. Bruno, and M. Conti, "RPL routing protocol in advanced metering infrastructures: An analysis of the unreliability problems," Proc. SustainIT, Oct. 2012.

[17] P. Levis, T. Clausen, J. Hui, O. Gnawali, and J. Ko, "The Trickle Algorithm," IETF RFC 6206, Mar. 2011.

Ryuichi Nagao is a candidate of the Ph.D. degree of Graduate School of Informatics, Kyoto University, Japan. He received the B.E. degree in Faculty of Engineering from the Kyoto University, Japan, in 2022, and the M.I. degree in Graduate School of Informatics, Kyoto University, Japan, in 2024. His current research topics include route construction methods and connection time reduction for wireless smart utility networks (Wi-SUN).

Daiki Hotta received the B.E. degree in Faculty of Engineering from the Kyoto University, Japan, in 2019, and the M.I. degree in Graduate School of Informatics, Kyoto University, Japan, in 2021. He researched low power and lossy multihop network protocols for wireless smart utility networks (Wi-SUN) in Kyoto university.

Hiroko Masaki is a researcher at Graduate School of Informatics, Kyoto University. She developed various software for communication systems such as mobile phones and car informatics at NEC IC Microcomputer Systems, Ltd. (currently Renesas Electronics Corporation) for over 20 years. From 2015 to 2017, she conducted research on social big data platform for railway infrastructure at YRP-IoT, Ltd. Then, from 2017 to 2019, she joined Japan Science and Technology Agency (JST), where she was involved in research and development of ultra big data platform integrating IoT wireless systems and databases. In 2019, she joined Graduate School of Informatics, Kyoto University as a researcher. Currently, she is engaged in research and development on IoT wireless communication systems based on IEEE 802.15.4 based Wireless Utility Network (Wi-SUN) at Kyoto University.

Keiichi Mizutani is an associate professor of the Graduate School of Informatics, Kyoto University. He received a B.E. degree in engineering from the Osaka Prefecture University, Japan, in 2007, and an M.E. and Ph.D. degree in engineering from the Tokyo Institute of Technology, Japan, in 2009 and 2012, respectively. He was an invited researcher at Fraunhofer Heinrich Hertz Institute, Germany, in 2010. From Apr. 2012 to Sept. 2014, he was a researcher at National Institute of Information and Communications Technology (NICT). From Oct. 2014 to Dec. 2021, he was an assistant professor of the Graduate School of Informatics, Kyoto University. From Jan. 2021 to Sep. 2022, he was an associate professor of the School of Platforms, Kyoto University (KUSP). He currently researches the topics of physical layer technologies in White Space Communications, Dynamic Spectrum Access, Wireless Smart Utility Networks (Wi-SUN), and 4G/5G/6G systems including OFDM, OFDMA, MIMO, multi-hop relay network, and full-duplex cellular systems. Since joining in NICT, he has been involved in IEEE 802 standardization activities, namely 802.11af, 802.15.4m and 802.22b. He received the Special Technical Awards from IEICE SR technical committee in 2009 and 2017, the Best Paper Award from IEICE SR technical committee in 2010 and 2020, the Young Researcher's Award from IEICE SRW technical committee in 2016, the Best Paper Award from WPMC2017 and WPMC2020, and the Best Paper Presentation Award (1st Place) from IEEE WF-IoT 2020.

Hiroshi Harada is a professor of the Graduate School of Informatics, Kyoto University, and an Research Executive Director of Wireless Networks Research Center, National Institute of Information and Communications Technology (NICT). He joined the Communications Research Laboratory, Ministry of Posts and Communications, in 1995 (currently, NICT). He was a Visiting Professor at the University of Electro-Communications, Tokyo, Japan, from 2005 to 2014. Since 1995, he has researched software defined radio, cognitive radio, dynamic spectrum access network, wireless smart utility network, and broadband wireless access systems on VHF, UHF, microwave, and millimeter-wave bands. In 2014, he was a professor at Kyoto University. He has also joined many standardization committees and forums in the United States as well as in Japan and fulfilled important roles in them, especially IEEE 1900 and IEEE 802. He was the chair of IEEE DySpan Standards Committee and a vice chair of IEEE 802.15.4g, 802.15.4m, 802.15.4aa, 1900.4a, 1900.4.1, and TIA TR-51. He was a board of directors of IEEE communication society standards board, SDR forum, DSA alliance, and WhiteSpace alliance. He is a Co-Founder of Wi-SUN alliance and has served as the chairman of the board from 2012 to 2019 and 2014. He is currently the Vice chair of IEEE 2857 and IEEE 802.15.4ad. Moreover, he was the chair of the IEICE Technical Committee on Software Radio (TCSR) and the chair of Public Broadband Mobile Communication Development Committee, ARIB. He is also involved in many other activities related to telecommunications. He authored the book titled “Simulation and Software Radio for Mobile Communications (Artech House, 2002).” He received the achievement awards in 2006 and 2018 and fellow of IEICE in 2009, respectively and the achievement awards of ARIB in 2009, 2018, and 2022, respectively, on the topic of research and development of cognitive radio and Wi-SUN.